

Relativistic effects on the imaging by a rotating optical system

Guillem Anglada¹, Sergei A. Klioner², Michael Soffel², and Jordi Torra¹

¹ Departament d'Astronomia i Meteorologia, Universitat de Barcelona, Av. Diagonal 647, 08028 Barcelona, Spain

² Lohrmann Observatory, Dresden Technical University, Mommsenstr. 13, 01062 Dresden, Germany

Received March 7, 2019/ Accepted March 7, 2019

Abstract. Special-relativistic effects on the imaging by a non-point-like arbitrarily moving optical instrument are discussed. Special-relativistic reflection law for a mirror of arbitrary shape and motion is derived in the limit of geometrical optics. In application to Gaia the effects of that relativistically modified reflection law of the images produced by a rotating reflector are demonstrated.

Key words. Astrometry – Reference systems – Relativity – Gaia

1. Introduction

The purpose of this paper is to investigate possible relativistic effects on the imaging by an optical system in arbitrary motion. Normally, in the framework of relativity one considers point-like observers. The methods to calculate observed quantities for such observers are well known. It is tacitly assumed herewith that the actual instrumentation of the observer is so small that one considers the positions and velocities of each part of the instrument to be the same (and that single position and velocity is called the position and velocity of the observer). In reality even for an Earth-based telescope it is clear that the velocities of different parts of the primary mirror in inertial coordinates (not rotating with the Earth) are slightly different. However, in the past the accuracy of observations was considered to be “too low” and the size of the mirror “too small” for that differences to be of practical relevance.

Due to recent technical developments especially for astrometric space missions like Gaia (de Boer et al. 2000; Perryman et al. 2001; Bienaymé & Turon 2002), JASMINE (Gouda et al. 2002) and SIM (Shao 1998) the situation has changed. In case of Gaia, we deal with a scanning satellite which permanently rotates in space with a period of 6 hours. The size of the primary mirror of Gaia is comparable with the size of the spacecraft itself. The goal best accuracy of Gaia is a few μas (and can be even below that limit in some favorable cases). Therefore, one cannot neglect a priori the difference of the velocities of various parts of the instruments. It is our purpose to investigate these effects and estimate their magnitude for Gaia.

The general-relativistic model for Gaia has been formulated in full detail by Klioner (2003, 2004). The model uses two principal relativistic reference systems: (1) Barycentric Celestial Reference System (BCRS) and (2) Center of Mass Reference System (CoMRS) of the satellite. The former is a global reference system with the origin at the barycenter of the solar system. It has been recommended by the International Astronomical Union for relativistic modelling of high-accuracy astronomical observations (Soffel et al. 2003). This reference system is used to model the dynamics of massive bodies, space vehicles (e.g. Gaia satellite) and light rays within the Solar system. The final Gaia catalogue will contain coordinates of celestial objects in the BCRS. The CoMRS is the local relativistic reference system of the satellite. It is explicitly constructed by Klioner (2004). The gravitational influence of massive bodies is effaced in the CoMRS as much as possible and, according to the equivalence principle, represented by tidal potentials. The CoMRS has its origin in the center of mass of the satellite and is kinematically non-rotating with respect to the BCRS. The CoMRS is physically adequate to model phenomena occurring in the immediate neighborhood of the satellite: attitude, the process of observation, etc. According to Klioner (2004) the metric tensor of the CoMRS differs from the Minkowski metric by three kinds of terms (the gravitational field of the satellite is too small and can be safely neglected): inertial term due to non-gravitational accelerations of the satellite (for Gaia these accelerations can be relatively large during orbital maneuvers and only about $2 \times 10^{-13} \text{ m/s}^2$ in between); inertial term due to slow rotation of the CoMRS relative to the instantaneously comoving Fermi-Walker transported locally inertial reference system (the angular velocity of that rotation $\sim 3 \times 10^{-15} \text{ s}^{-1} = 2''$ per century); and tidal

gravitational potentials (they produce relative acceleration of at most 10^{-12} m/s² at a distance of 2.5 meters from the satellite's center of mass). Simple calculations show that all these terms influence the CoMRS light propagation within a few meters from the satellite's center of mass at a level much lower than the goal accuracy of 1 μ s. Therefore, all these terms can be neglected for our purposes and one can consider the CoMRS as an inertial reference system of Special Relativity.

In this paper we confine ourselves to the case where the optical instrument consists only of mirrors (no lens). In Section 3 as a co-product of this investigation we derive a general Special-relativistic reflection law for an arbitrarily moving mirror. In Section 4 the effect of this Special-relativistic reflection law on the imaging by a rotating telescope is investigated.

At the end of Section 4 we sketch some questions that remain open about the real image formation process and how some phase aspects of the light propagation may affect the astrometric measurements. Detailed wave optics calculations will ultimately be required to solve that open issues.

2. Notation and conventions

Let us summarize the most important notation and conventions used throughout the paper:

- c is the velocity of light in vacuum.
- Lowercase latin indices a, i, j, \dots take values 1, 2, 3 and refer to spatial components of corresponding quantities.
- The index 0 is used for time components.
- Greek indices α, μ, ν, \dots take values 0, 1, 2 and 3 and refer to all space-time components of corresponding quantities.
- The Minkowski metric is denoted by $\eta = \text{diag}(-1, +1, +1, +1)$.
- All the latin indices are lowered and raised by means of the unit matrix $\delta_{ij} = \delta^{ij} = \text{diag}(1, 1, 1)$, and therefore the disposition of such indices plays no role: $a^i = a_i$.
- The symbol ε_{ijk} is the fully antisymmetric Levi-Civita symbol ($\varepsilon_{123} = +1$).
- Repeated indices imply Einstein summation rule irrespective of their positions (e.g., $a_i b_i = a_1 b_1 + a_2 b_2 + a_3 b_3$).
- The spatial components of a quantity considered as a 3-vector are set in boldface: $\mathbf{a} = a^i$.
- The absolute value (Euclidean norm) of a 3-vector \mathbf{a} is denoted $|\mathbf{a}|$ and is defined by $|\mathbf{a}| = (a^1 a^1 + a^2 a^2 + a^3 a^3)^{1/2}$.
- The scalar product of any two 3-vectors \mathbf{a} and \mathbf{b} with respect to the Euclidean metric δ_{ij} is denoted by $\mathbf{a} \cdot \mathbf{b}$ is defined by $\mathbf{a} \cdot \mathbf{b} = \delta_{ij} a^i b^j = a^i b^i$.

Below two reference systems (t, x^i) and (T, X^a) will be used. To improve readability of the formulas all quantities

defined in $x^\mu = (t, x^i)$ are denoted by small latin characters with space-time and spatial indices taken from second parts of the Greek and Latin alphabet, respectively $(\mu, \nu, \dots, i, j, \dots)$. All quantities defined in $X^\alpha = (T, X^a)$ are denoted by capital latin characters with space-time and spatial indices taken from first parts of the Greek and Latin alphabet, respectively $(\alpha, \beta, \dots, a, b, \dots)$.

3. Reflection of a light ray on an arbitrarily moving mirror

Let us first consider a simple problem within the framework of Special Relativity. Given a mirror in arbitrary motion and a light ray hitting the surface of the mirror at a given point and moment of time we would like to calculate the parameters of the outgoing light ray. Clearly we will work in the usual limit of geometrical optics. The simplified problem of a plain mirror moving with a constant velocity perpendicular to its surface has been considered by Einstein (1905). We consider here the most general case of this problem within Special Relativity. A comparison with the results known from the literature will be given below.

Slightly modifying the arguments of Einstein (1905) we first use Lorentz transformations to transform from a laboratory inertial reference system (t, x^i) to an inertial reference system (T, X^a) instantaneously co-moving with the point of the mirror where the reflection occurs, then apply the known reflection law in that reference system and transform the reflected light ray back into the laboratory reference system. The relation of that scheme to direct calculations with Maxwell equations is discussed below.

3.1. Coordinate representation of an arbitrary moving mirror

Let us consider an inertial reference system of Special Relativity (t, x^i) . We define an arbitrary mirror in arbitrary motion by a bundle of particles moving along world-lines

$$x_m^\mu(t; \xi, \eta) = (t, x_m^i(t; \xi, \eta)). \quad (1)$$

here ξ and η are two parameters “numbering” the particles. These parameters can be thought of as some non-degenerated coordinate system on the surface of the mirror which is described by $x_m^i(t; \xi, \eta)$ for any fixed time t . We assume that $x_m^i(t; \xi, \eta)$ is differentiable with respect to all its three parameters.

Here we do not pay attention to any physical properties of the mirror as a “physical body” (elasticity, deformations, etc.). We just consider that (1) formally defines the position of each point of the mirror at each moment of time. Starting from (1) it is easy to see that for any fixed time t at any fixed point of the mirror characterized by some values of ξ and η we have two three-dimensional vectors tangent to the surface of the mirror at the considered point as

$$l^i = \frac{\partial}{\partial \xi} x_m^i(t, \xi, \eta), \quad (2)$$

$$m^i = \frac{\partial}{\partial \eta} x_m^i(t, \xi, \eta). \quad (3)$$

Then a vector normal to the surface of the mirror at that point can be calculated as

$$n^i = \varepsilon_{ijk} l^j m^k. \quad (4)$$

The order of vectors l^i and m^i in (4) is arbitrary and corresponds to a choice of the sign in the definition of n^i (if n^i is a normal vector then $-n^i$ is also a normal). Not restricting the generality we assume below that (4) defines that n^i which is directed toward the “working surface” of the mirror. On the other hand, the coordinate velocity of any point of the mirror reads

$$v_m^i = \frac{\partial}{\partial t} x_m^i(t, \xi, \eta). \quad (5)$$

3.2. Transforming the mirror surface from one inertial reference system to another

Let us now define another reference system (T, X^a) moving with constant velocity v^i with respect to (t, x^i) . The coordinates (T, X^a) and (t, x^i) are related by a Lorentz transformation of the form

$$ct = \mathbf{L}_0^0 cT + \mathbf{L}_a^0 X^a, \quad (6)$$

$$x^i = \mathbf{L}_0^i cT + \mathbf{L}_a^i X^a. \quad (7)$$

The \mathbf{L} matrix coefficients are given by

$$\mathbf{L}_0^0 = \gamma, \quad (8)$$

$$\mathbf{L}_a^0 = k^a \gamma, \quad (9)$$

$$\mathbf{L}_0^i = k^i \gamma, \quad (10)$$

$$\mathbf{L}_a^i = \delta^{ia} + \frac{\gamma^2}{1 + \gamma} k^i k^a, \quad (11)$$

$$\gamma = (1 - \mathbf{k} \cdot \mathbf{k})^{-\frac{1}{2}}, \quad (12)$$

$$\mathbf{k} = \frac{1}{c} \mathbf{v}. \quad (13)$$

The inverse transformation reads

$$cT = \bar{\mathbf{L}}_0^0 ct + \bar{\mathbf{L}}_i^0 x^i, \quad (14)$$

$$X^a = \bar{\mathbf{L}}_0^a ct + \bar{\mathbf{L}}_i^a x^i. \quad (15)$$

with

$$\bar{\mathbf{L}}_0^0 = \gamma, \quad (16)$$

$$\bar{\mathbf{L}}_i^0 = -k^i \gamma, \quad (17)$$

$$\bar{\mathbf{L}}_0^a = -k^a \gamma, \quad (18)$$

$$\bar{\mathbf{L}}_i^a = \delta^{ia} + \frac{\gamma^2}{1 + \gamma} k^i k^a. \quad (19)$$

Clearly, in the reference system (T, X^a) the mirror can be also represented in the same form as in Section 3.1

$$X_m^a(T, \xi, \eta) = (T, X_m^a(T, \xi, \eta)), \quad (20)$$

where fixed values for ξ and η should correspond to one and the same surface particle in both coordinate systems.

The vectors tangent and normal to the surface read

$$L^a = \frac{\partial}{\partial \xi} X_m^a(T, \xi, \eta), \quad (21)$$

$$M^a = \frac{\partial}{\partial \eta} X_m^a(T, \xi, \eta), \quad (22)$$

$$N^a = \varepsilon_{abc} L^b M^c. \quad (23)$$

Again the velocity of a point of the mirror is given by

$$V_m^a = \frac{\partial}{\partial T} X_m^a(T, \xi, \eta). \quad (24)$$

In order to relate the vectors L^a , M^a , N^a and V_m^a to the corresponding ones in the reference system (t, x^i) we consider the coordinate transformation of the events defined by (1) and (20)

$$cT = \bar{\Lambda}_0^0 ct + \bar{\Lambda}_i^0 x_m^i(t, \xi, \eta), \quad (25)$$

$$X_m^a(T, \xi, \eta) = \bar{\Lambda}_0^a ct + \bar{\Lambda}_i^a x_m^i(t, \xi, \eta). \quad (26)$$

The function $X_m^a(T, \xi, \eta)$ is thus defined by (25)–(26) implicitly since (25) should be inverted to give t as function of T , ξ and η and that t should be substituted into (26) to give the explicit dependence of X_m^a on T , ξ and η . Clearly, that inversion cannot be done explicitly for any $x_m^i(t, \xi, \eta)$. However, the partial derivatives L^a , M^a and V_m^a of $X_m^a(T, \xi, \eta)$ can be calculated as derivatives of an implicit function. A straightforward algebra gives

$$V_m^a = c \frac{\bar{\Lambda}_0^a + \bar{\Lambda}_i^a k_m^i}{\bar{\Lambda}_0^0 + \bar{\Lambda}_i^0 k_m^i}, \quad (27)$$

$$L^a = \bar{S}_i^a l^i \quad (28)$$

$$M^a = \bar{S}_i^a m^i \quad (29)$$

$$\bar{S}_i^a = \bar{\Lambda}_i^a - \bar{\Lambda}_0^0 \frac{\bar{\Lambda}_0^a + \bar{\Lambda}_j^a k_m^j}{\bar{\Lambda}_0^0 + \bar{\Lambda}_j^0 k_m^j}, \quad (30)$$

or inverting

$$v_m^i = c \frac{\mathbf{L}_0^i + \mathbf{L}_a^i K_m^a}{\mathbf{L}_0^0 + \mathbf{L}_a^0 K_m^a}, \quad (31)$$

$$l^i = S_a^i L^a, \quad (32)$$

$$m^i = S_a^i M^a, \quad (33)$$

$$S_a^i = \mathbf{L}_a^i - \mathbf{L}_a^0 \frac{\mathbf{L}_0^i + \mathbf{L}_b^i K_m^b}{\mathbf{L}_0^0 + \mathbf{L}_b^0 K_m^b}, \quad (34)$$

with $k_m^i = c^{-1} v_m^i$ and $K_m^a = c^{-1} V_m^a$. Equations (27) and (31) coincide with the law for velocities addition in Special Relativity. One can also check by direct calculation that $S_a^i \bar{S}_j^a = \delta_j^i$ and $\bar{S}_i^a S_b^a = \delta_b^i$.

Using (30) and (34) one can see that

$$\bar{S}_j^b \bar{S}_k^c \varepsilon_{abc} = \frac{1}{\gamma(1 - \mathbf{k} \cdot \mathbf{k}_m)} S_a^i \varepsilon_{ijk}, \quad (35)$$

$$S_b^j S_c^k \varepsilon_{ijk} = \gamma(1 - \mathbf{k} \cdot \mathbf{k}_m) \bar{S}_i^a \varepsilon_{abc}. \quad (36)$$

Now using these formulas, definitions (23) and (4) and relations (28)–(29) and (32)–(33) one can prove that N^a and n^i are related as

$$N^a = \frac{1}{\gamma(1 - \mathbf{k} \cdot \mathbf{k}_m)} S_a^i n^i, \quad (37)$$

$$n^i = \gamma(1 - \mathbf{k} \cdot \mathbf{k}_m) \bar{S}_i^a N^a. \quad (38)$$

To proof (35)–(36) we used the identity

$$\varepsilon_{ajc} \delta^{kb} + \varepsilon_{kac} \delta^{jb} + \varepsilon_{jkc} \delta^{ab} = \varepsilon_{ajk} \delta^{bc}. \quad (39)$$

The relations between N^a and n^i will be used below for the particular case when the velocity v^i of the reference system (T, X^a) relative to (t, x^i) coincides with the velocity v_m^i of a particular point of the mirror at some given moment of time (that is, from now on we put $\mathbf{k}_m = \mathbf{k}$). Normalizing the vectors one can see that the normal unit vector $\hat{N} = \mathbf{N}/|\mathbf{N}|$ to the surface as seen by an observer instantaneously co-moving with a particular point of the mirror relates to the normal unit vector $\hat{n} = \mathbf{n}/|\mathbf{n}|$ seen by an observer at rest relative to (t, x^i) as

$$\hat{N} = \frac{1}{\sqrt{1 - (\mathbf{k} \cdot \hat{n})^2}} \left(\hat{n} - (\mathbf{k} \cdot \hat{n}) \frac{\gamma}{1 + \gamma} \mathbf{k} \right), \quad (40)$$

$$\hat{n} = \frac{1}{\sqrt{1 + \gamma^2 (\mathbf{k} \cdot \hat{N})^2}} \left(\hat{N} + (\mathbf{k} \cdot \hat{N}) \frac{\gamma^2}{1 + \gamma} \mathbf{k} \right). \quad (41)$$

It is illustrative to see that this transformation of normal vectors can be derived by the transformation rule of 4-vectors. Let us consider a certain surface element in its instantaneously co-moving inertial coordinate system (T, X^a) . In that system we consider the 3-components of the surface normal vector \hat{N} as spatial components of the 4-vector $\hat{N}_\alpha = (0, \hat{N}^a)$. A Lorentz transformation of this 4-vector to coordinates (t, x^i) leads to result (41) after normalization.

3.3. Wave vectors in different inertial reference systems

In the reference system (t, x^i) the incoming light ray is characterized by its null wave vector p^μ ($\eta_{\mu\nu} p^\mu p^\nu = 0$). The unit light ray direction σ^i ($\boldsymbol{\sigma} \cdot \boldsymbol{\sigma} = 1$) in that reference system is related to p^μ as $\sigma^i = p^i/p^0$. In the reference system (T, X^a) the null wave vector of the same light ray is P^α , and the unit light ray direction $\Sigma^a = P^a/P^0$ ($\boldsymbol{\Sigma} \cdot \boldsymbol{\Sigma} = 1$). The frequencies f and F of the light in the corresponding reference systems are linearly proportional to p^0 and P^0 , respectively.

The wave vectors p^μ and P^α are related by the Lorentz transformation

$$P^\alpha = \bar{\Lambda}_\mu^\alpha p^\mu, \quad (42)$$

$$p^\mu = \mathbf{L}_\alpha^\mu P^\alpha, \quad (43)$$

which means that the frequencies and unit light ray directions are related as

$$\Sigma^a = \frac{\bar{\Lambda}_0^a + \bar{\Lambda}_i^a \sigma^i}{\bar{\Lambda}_0^0 + \bar{\Lambda}_i^0 \sigma^i}, \quad (44)$$

$$\sigma^i = \frac{\Lambda_0^i + \Lambda_a^i \Sigma^a}{\Lambda_0^0 + \Lambda_a^0 \Sigma^a}, \quad (45)$$

$$F = \left(\bar{\Lambda}_0^0 + \bar{\Lambda}_i^0 \sigma^i \right) f, \quad (46)$$

$$f = \left(\Lambda_0^0 + \Lambda_a^0 \Sigma^a \right) F. \quad (47)$$

3.4. Reflection as seen by an instantaneously co-moving observer

For an observer instantaneously co-moving with the point of the mirror where the light ray is reflected; the following simple reflection law is valid (in an inertial reference system of Special Relativity for a mirror at rest),

$$F' = F, \quad (48)$$

$$\boldsymbol{\Sigma}' = \boldsymbol{\Sigma} - 2(\hat{N} \cdot \boldsymbol{\Sigma}) \hat{N}, \quad (49)$$

where \hat{N} is the unit normal vector to the surface of the mirror at the point of reflection. The reflection law (49) means simply that the component of $\boldsymbol{\Sigma}$ perpendicular to the surface changes its sign. This is equivalent to say that the angle of incidence is equal to the angle of reflection and that the incoming ray $\boldsymbol{\Sigma}$, the reflected ray $\boldsymbol{\Sigma}'$ and the normal \hat{N} are coplanar. The same equations (48) and (49) are valid for, respectively, time and space components of wave vectors before and after reflection.

We consider this reflection law as given, but it is well known how to derive it from Maxwell equations for electromagnetic field for a mirror at rest (Jackson 1975). In the instantaneously co-moving reference system (T, X^a) the coordinate velocity of the reflecting point vanishes but its acceleration may differ from zero. However, the acceleration cannot affect the instantaneous process of reflection in virtue of the equivalence principle as long as the conditions for geometrical optics are satisfied (see also Section 3.8 below).

3.5. Reflection as seen by a laboratory observer

Now combining the reflection law in reference system (T, X^a) with the transformations discussed in Sections 3.2–3.3 one gets the reflection law as seen in reference system (t, x^i) where the mirror is arbitrarily moving

$$f' = f \frac{1 + (\mathbf{k} \cdot \hat{n}) [\hat{n} \cdot (\mathbf{k} - 2\boldsymbol{\sigma})]}{1 - (\mathbf{k} \cdot \hat{n})^2}, \quad (50)$$

$$\boldsymbol{\sigma}' = \frac{\left(1 - (\mathbf{k} \cdot \hat{n})^2\right) \boldsymbol{\sigma} + 2(\mathbf{k} \cdot \hat{n} - \boldsymbol{\sigma} \cdot \hat{n}) \hat{n}}{1 + (\mathbf{k} \cdot \hat{n})^2 - 2(\mathbf{k} \cdot \hat{n})(\boldsymbol{\sigma} \cdot \hat{n})}. \quad (51)$$

Here, f' and $\boldsymbol{\sigma}'$ are the frequency and the unit direction of the reflected light ray in the reference system (t, x^i) . These expressions are valid at each point of the mirror surface in arbitrary motion. Let us remind that $\mathbf{k} = \mathbf{v}_m/c$, where \mathbf{v}_m is the coordinate velocity of the reflecting point of the mirror at the moment of reflection. Velocity \mathbf{v}_m can be computed from any mathematical representation of the mirror surface (for example, from (5)).

The same way can be used to derive the 4-momentum or 4-velocity of a particle p^μ after a completely elastic collision with a surface of infinite mass:

$$p'^0 = p^0 - 2\mathbf{k} \cdot \hat{\mathbf{n}} \left(\frac{\mathbf{p} \cdot \hat{\mathbf{n}} - \mathbf{k} \cdot \hat{\mathbf{n}} p^0}{1 - (\mathbf{k} \cdot \hat{\mathbf{n}})^2} \right), \quad (52)$$

$$p'^i = p^i - 2\hat{n}^i \left(\frac{\mathbf{p} \cdot \hat{\mathbf{n}} - \mathbf{k} \cdot \hat{\mathbf{n}} p^0}{1 - (\mathbf{k} \cdot \hat{\mathbf{n}})^2} \right), \quad (53)$$

where p^μ is wave vector of the particle before the collision. Recalling the relations between wave vectors and frequencies and directions for a photon it is easy to see that Eqs. (52)–(53) are equivalent to (50)–(51).

Let us note two important properties of (50)–(51), also applicable to (52)–(53).

- Also in the reference system (t, x^i) the reflected direction σ' lies in the plane defined by the incoming ray σ and the normal vector $\hat{\mathbf{n}}$.
- The reflected ray is only affected by the projection of the velocity \mathbf{v}_m on the local $\hat{\mathbf{n}}$ vector.

The latter property implies that the relation between σ' and σ coincides with the usual reflection law (49) if the velocity \mathbf{v}_m is perpendicular to $\hat{\mathbf{n}}$. This case is relevant for liquid (rotating) mirrors and was discussed by Lightman et al. (1975, problem 1.19), Ragazzoni & Claudi (1995) and Hickson et al. (1995). Our result (no relativistic effects on reflection law in that case) coincides with that of Lightman et al. (1975) and Hickson et al. (1995).

Multiplying both sides of (51) by $\hat{\mathbf{n}}$ and use the following definitions for the angles between vectors

$$-\sigma \cdot \hat{\mathbf{n}} = \cos \alpha, \quad (54)$$

$$\sigma' \cdot \hat{\mathbf{n}} = \cos \alpha', \quad (55)$$

$$\mathbf{k} \cdot \hat{\mathbf{n}} = k \cos \left(\varphi - \frac{\pi}{2} \right) = k \sin \varphi, \quad (56)$$

($k = |\mathbf{k}| = |\mathbf{v}_m|/c$) one obtains a relation between the angle of incidence α and angle of reflection α'

$$f' = f \frac{1 + 2k \sin \varphi \cos \alpha + k^2 \sin^2 \varphi}{1 - k^2 \sin^2 \varphi}, \quad (57)$$

$$\cos \alpha' = \frac{2k \sin \varphi + (1 + k^2 \sin^2 \varphi) \cos \alpha}{1 + k^2 \sin^2 \varphi + 2k \sin \varphi \cos \alpha}. \quad (58)$$

The latter equation can be also re-written into an equation relating $\sin \alpha$ and $\sin \alpha'$ (note that this form contains the same factor as (57)):

$$\sin \alpha' = \sin \alpha \frac{1 - k^2 \sin^2 \varphi}{1 + 2k \sin \varphi \cos \alpha + k^2 \sin^2 \varphi}. \quad (59)$$

Angles α , α' and φ are illustrated on Fig. 1. The angle α lies between 0 and $\pi/2$ (since we always consider that the incoming light ray comes to the mirror from one particular side of the tangent plane to the mirror's surface at the

point of reflection). For the same reason we have $0 \leq \alpha' \leq \pi/2$. Angle φ lies between $-\pi/2$ and $\pi/2$. It is negative if the angle between \mathbf{k} and $\hat{\mathbf{n}}$ is greater than $\pi/2$ and positive otherwise.

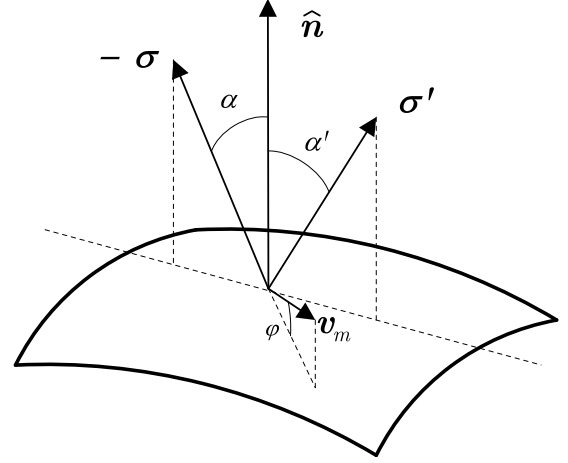


Fig. 1. Vectors and angles at the reflection point. The vector $\hat{\mathbf{n}}$ is a unit vector perpendicular to the surface of the mirror at the reflection point. Vectors σ and σ' are unit directions of propagation of the incoming and reflected light rays, respectively. The vector \mathbf{v}_m is the velocity of the point of the mirror at which the reflection occurs. The symbol α ($0 \leq \alpha \leq \pi/2$) is the angle between the direction $-\sigma$ toward the source of the incoming light ray and vector $\hat{\mathbf{n}}$. The symbol α' ($0 \leq \alpha' \leq \pi/2$) is the angle between the propagation direction σ' of the reflected light ray and vector $\hat{\mathbf{n}}$. Finally φ ($-\pi/2 \leq \varphi \leq \pi/2$) is the angle between the velocity vector \mathbf{v}_m and the plane tangential to the mirror at the point of reflection. The latter angle is negative if the angle between \mathbf{v}_m and $\hat{\mathbf{n}}$ is greater than $\pi/2$ and positive otherwise. Because of the Special-relativistic effects angle α and α' are in general different.

3.6. Particular case of a flat mirror moving with a constant velocity

As a particular example let us apply the developed scheme to a flat mirror moving at constant velocity in reference frame (t, x^i) . The mathematical expression for that is a worldline equation (1) in the form

$$\mathbf{x}_m(t, \xi, \eta) = \mathbf{x}_{m0} + \mathbf{l} \xi + \mathbf{m} \eta + \mathbf{v}_m t, \quad (60)$$

where \mathbf{l} , \mathbf{m} , \mathbf{v}_m and \mathbf{x}_{m0} are constant vectors defining position, velocity and orientation of the mirror. It is easy to see that in coordinates (T, X^a) one gets

$$\mathbf{X}_m(T, \xi, \eta) = \mathbf{X}_{m0} + \mathbf{L} \xi + \mathbf{M} \eta + \mathbf{V}_m T, \quad (61)$$

where vectors \mathbf{V}_m , \mathbf{L} and \mathbf{M} are related to \mathbf{v}_m , \mathbf{l} and \mathbf{m} by (27), (28) and (29), respectively, and $X_{m0}^a = \tilde{S}_i^a x_{m0}^i$. Eq. (61) implies that a flat surface remains flat in any inertial reference system.

Since for a flat mirror \mathbf{l} and \mathbf{m} are constants, the unit normal vector $\hat{\mathbf{n}}$ is also a constant. Since \mathbf{v}_m is also time-independent the same reflection law (51) and (58) are valid for any point of the mirror and at any moment of time. One can check that (58) coincides with the results of Gjurchinovski (2004). We believe, however, that our framework is more general than that of Gjurchinovski (2004) since we do not *assume* the vectors $\boldsymbol{\sigma}$, $\hat{\mathbf{n}}$, \mathbf{k} and $\hat{\mathbf{s}}$ to be all coplanar, and we derive the same formula for an arbitrary mirror in arbitrary motion.

Note that the central result of Gjurchinovski (2004) coincides with the formula derived by Einstein (1905) in the particular case of a flat mirror moving with constant velocity directed perpendicular to the surface when $\sin \varphi = 1$ (see also Lightman et al. (1975, problem 1.18)). Bolotovskii & Stolyarov (1989a) have derived the same relation as Einstein (1905) by solving Maxwell field equations directly in the coordinates where the mirror is moving.

3.7. Low velocity limit

It is useful to derive the first-order expansion of (50)–(58) in powers of v_m/c since in practice the velocity of the mirror will be small compared to the velocity of light. One gets

$$f' = f (1 - 2(\boldsymbol{\sigma} \cdot \hat{\mathbf{n}})(\mathbf{k} \cdot \hat{\mathbf{n}}) + \mathcal{O}(c^{-2})), \quad (62)$$

$$\begin{aligned} \boldsymbol{\sigma}' &= \boldsymbol{\sigma} - 2(\boldsymbol{\sigma} \cdot \hat{\mathbf{n}})\hat{\mathbf{n}} \\ &+ 2(\mathbf{k} \cdot \hat{\mathbf{n}}) [(1 - 2(\boldsymbol{\sigma} \cdot \hat{\mathbf{n}})^2)\hat{\mathbf{n}} + (\boldsymbol{\sigma} \cdot \hat{\mathbf{n}})\boldsymbol{\sigma}] \\ &+ \mathcal{O}(c^{-2}), \end{aligned} \quad (63)$$

or

$$f' = f (1 + 2k \sin \varphi \cos \alpha + \mathcal{O}(c^{-2})), \quad (64)$$

$$\cos \alpha' = \cos \alpha + 2k \sin \varphi \sin^2 \alpha + \mathcal{O}(c^{-2}), \quad (65)$$

$$\sin \alpha' = \sin \alpha - k \sin \varphi \sin 2\alpha + \mathcal{O}(c^{-2}). \quad (66)$$

The first two terms in the right-hand side of (63) represent just the usual reflection law and the rest contains the largest relativistic effects. Eq. (65) shows that

$$\alpha' - \alpha = -2k \sin \varphi \sin \alpha + \mathcal{O}(c^{-2}). \quad (67)$$

This expression can be used to estimate the difference $\alpha' - \alpha$ for many realistic situations.

3.8. Derivation of results by means of Maxwell's equations

It is illustrative to see how the results (57)–(58) can be derived directly from Maxwell's equations. It is well known that the usual reflection law can be obtained from Maxwell's theory by a principle of phase matching: the

phase of the incoming wave Φ should agree with the phase of the outgoing wave Φ' on the mirror surface m (e.g., Jackson (1975, Section 7.3)):

$$\Phi|_m = \Phi'|_m. \quad (68)$$

The central results (57)–(58) can simply be derived from the principle of phase matching in case of a flat mirror moving with constant velocity \mathbf{v}_m with respect to inertial coordinates x^μ where the observer is at rest. The mirror x_m^i is given in this case by (60). The constant (time- and position-independent) unit normal vector is again denoted as $\hat{\mathbf{n}}$. Maxwell's equations in inertial coordinates lead to the usual wave equation of the form

$$-\left(\frac{1}{c^2} \frac{\partial^2}{\partial t^2} + \Delta\right) \Psi = 0 \quad (69)$$

that is solved, e.g., by a monochromatic plane wave of the form

$$\Psi = a \exp(i p_\mu x^\mu) \equiv a \exp(i \Phi) \quad (70)$$

with a wave vector $p^\mu = (p^0, \mathbf{p})$ satisfying the usual null condition

$$-p^0 p^0 + \mathbf{p} \cdot \mathbf{p} = 0. \quad (71)$$

The principle of phase matching (68) then determines both the law of reflection and the Doppler shifts of “photon” frequencies. Let us decompose the wave vector \mathbf{p} into a tangential and a normal part with respect to the surface normal:

$$\mathbf{p} = \mathbf{p}_T + p_n \hat{\mathbf{n}}, \quad (72)$$

$$\mathbf{p}_T = \hat{\mathbf{n}} \times (\mathbf{p} \times \hat{\mathbf{n}}), \quad (73)$$

$$p_n = \mathbf{p} \cdot \hat{\mathbf{n}}. \quad (74)$$

Then phase matching on the mirror surface leads to

$$\mathbf{p}_T = \mathbf{p}'_T \quad (75)$$

$$p^0 - \frac{1}{c} \mathbf{v}_m \cdot \hat{\mathbf{n}} p_n = p'^0 - \frac{1}{c} \mathbf{v}_m \cdot \hat{\mathbf{n}} p'_n. \quad (76)$$

or using the null condition the two matching equations for frequencies f and f' and direction angles α and α' (see Fig. 1) take the form

$$f \sin \alpha = f' \sin \alpha' \quad (77)$$

$$f \left(1 + \frac{1}{c} \mathbf{v}_m \cdot \hat{\mathbf{n}} \cos \alpha\right) = f' \left(1 - \frac{1}{c} \mathbf{v}_m \cdot \hat{\mathbf{n}} \cos \alpha'\right). \quad (78)$$

Straightforward algebra then leads to the results (57) and (58) above. Note, that this phase-matching argument works in a simple way for plane mirrors and plane waves that mathematically are infinitely extended both in space and time. Such a treatment, however, is meaningful for any mirror as long as the conditions for geometrical optics are satisfied, i.e., as long as amplitude, polarization and wave vector do not change significantly over a distance determined by the wavelength. This implies that the acceleration a_m of the mirror should satisfy a constrain of the form $a_m \ll c^2/\lambda$, where λ is the wavelength of the radiation.

4. Relativistic astrometric effects due to rotational motion of the satellite

For an optical system consisting solely of a number of arbitrarily moving mirrors, the Special-relativistic change of the reflection law will produce a change in aberration patterns as compared to the patterns calculated using normal Newtonian reflection law. These perturbed aberration patterns will certainly affect the astrometric measurements based on an interpretation of the images measured in the instrument's focal plane. To show that, let us consider an optical system rotating rigidly with a constant angular velocity relative to the inertial reference system (t, x^i) .

The shapes of the mirrors in coordinates (t, x^i) defined by $x_m^i(t; \xi, \eta)$ are assumed to be *given*. Here we do not consider the question of deformation of the mirrors due to their rotational motions (i.e., the relation between the intended shapes of the mirrors during their manufacturing and their shapes in rotating satellite in coordinates (t, x^i)). A rigorous relativistic treatment of this question would require at least a Special-relativistic theory of elasticity. As long as the angular velocity is constant the deformations are also constant and a rigidly rotating mirror can be considered to be Born-rigid (Pauli 1958, Section 45). We can also argue that the constant deformations are assumed to be properly taken into account during manufacturing so that the rotating mirrors have the assumed forms. For a scanning astrometric satellite the real angular velocity is not constant (e.g., because of its scanning law), but its change is small and slow, and can be neglected here.

To calculate the aberration patterns of several optical systems discussed below we have developed a numerical ray tracing code in Java allowing us to calculate aberration patterns for an arbitrary rigidly rotating optical system. Each mirror in the system can be individually shaped and oriented. The code allows us to control all intermediate calculations as well as the overall numerical accuracy.

Parameters of the optical systems (size of the mirrors, focal distance, distance of the primary mirror from the rotational axis and angular velocity) considered in Sections 4.1 and 4.2 below are chosen to represent qualitatively some principal features of planned astrometric missions like Gaia (Perryman et al. 2001) or JASMINE (Gouda et al. 2002), where a scanning satellite comprising two astrometric telescopes continuously rotates with an angular velocity of order $\Omega \sim 60''/\text{s}$.

4.1. One-mirror optical system

The first optical system that we will study is simple one rotating parabolic mirror. A scheme of this optical system is given on Fig. 2. The parabolic mirror M_1 is a square mirror of size $1.5 \text{ m} \times 1.5 \text{ m}$ and focal length $d_f = 46.67 \text{ m}$. This roughly corresponds to the astrometric instruments of Gaia. The receiver at the focal plane is considered to be $0.814 \text{ m} \times 0.814 \text{ m}$ providing a field of view of $\sim 1^\circ \times 1^\circ$. The rotational axes goes through the origin O of our coordinates perpendicular to the plane of Fig. 2. The distance

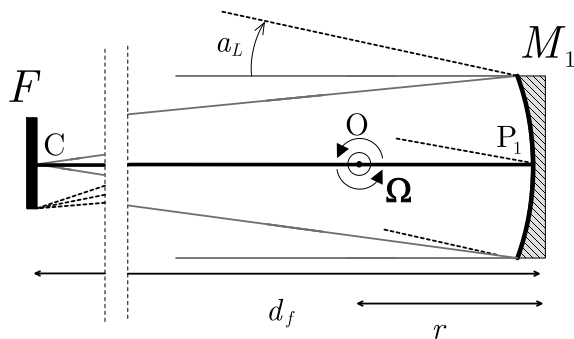


Fig. 2. A rotating optical system with one mirror. The primary mirror M_1 is parabolic. The point P_1 lies on the vertex of the parabola. The distance from the origin O to P_1 is r . The distance from P_1 to the focal plane center C is the focal distance of the parabola d_f . The optical system rotates rigidly around the origin O with an angular velocity Ω in the sense shown on the scheme. The direction of the incoming light ray is parameterized with two angles: the *along scan* angle a_L in the plane of the depicted scheme (this angle is changing continuously for a given source because of the rotation), and the *across scan* angle a_C (not shown in the picture) in the perpendicular direction. The instantaneous optical axis is represented by the bold horizontal line going from P_1 to C . Without rotation light rays parallel to the optical axis converge to the single point C in the focal plane.

from O to the center of the primary mirror P_1 is $r = 1.5 \text{ m}$. The distance from P_1 to the center of the focal plane C is obviously the focal distance 46.67 m . The whole optical system is rotating with respect to O with an angular velocity $\Omega = 60''/\text{s}$. The *optical axis* of the system is defined as the path of the light ray which goes perpendicular to the surface of the primary mirror through its center provided that the system does not rotate. The direction of an incoming light ray is parameterized with two angles: the *along scan* angle a_L and the *across scan* angle a_C (Fig. 2). The along scan angle is the angle between the instantaneous directions of the optical axis and the incoming light ray projected into the plane containing the optical axes and perpendicular the vector of angular velocity of the system. The across scan angle is the angle between the instantaneous directions of the optical axis and the incoming light ray projected into the plane containing both the optical axis and the vector of angular velocity. The along scan and across scan angles are widely used in the context of scanning astrometric missions like HIPPARCOS (Perryman et al. 1997) and Gaia (Perryman et al. 2001).

In order to evaluate the relativistic effects we compute the difference of the focal plane coordinates of the photocenters produced by the relativistic reflection law and the Newtonian one for different a_L and a_C . The differences in the focal plane coordinates can be easily recomputed into shifts δa_L and δa_C in the observed direction. To compute the photocenters a rectangular grid of parallel

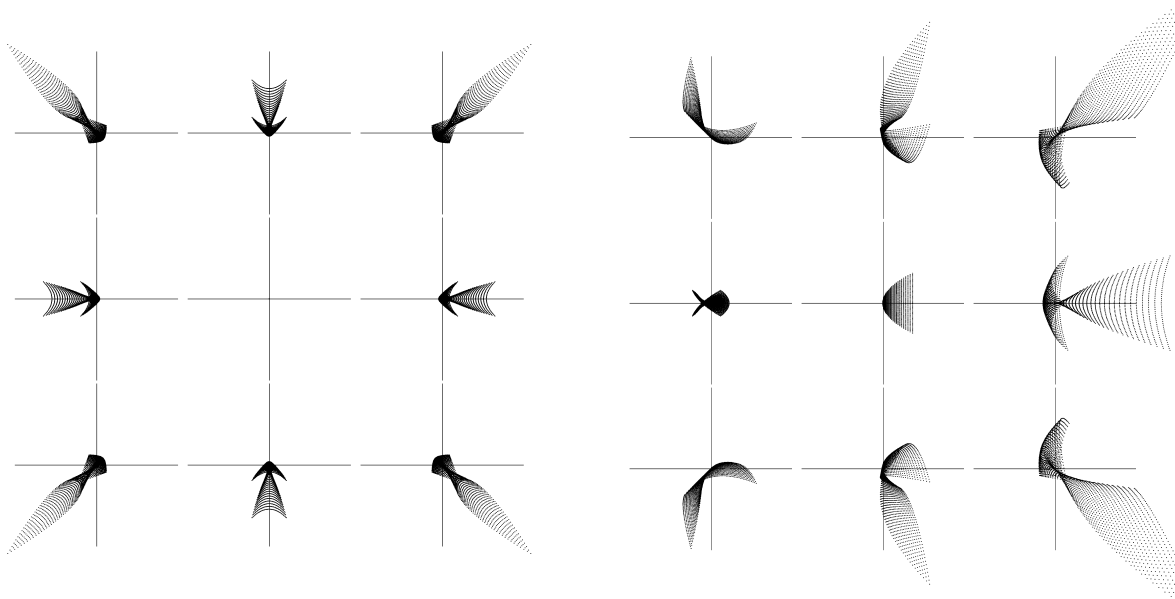


Fig. 3. Aberration patterns for a single parabolic mirror. The nine patterns are obtained using nine combinations of the field angles with $a_L = -30', 0', +30'$ (horizontal direction) and $a_C = -30', 0', +30'$ (vertical direction). For a focal length $d_f = 46.67$ m, $30'$ correspond to about 407 mm in the focal plane coordinates. The size of the axes in focal plane coordinates is $0.5 \text{ mm} \times 0.5 \text{ mm}$ in all sub-figures. The aberration patterns on the left panel are calculated for a non-rotating instrument (i.e. with the normal Newtonian reflection law). On the right pane the aberration patterns are obtained for an extremely high angular velocity $\Omega = 50000 \text{ s}^{-1}$. This angular velocity was chosen to exaggerate the distortion and make it clearly visible. In all cases the axes are centered at the image of the incoming light ray which goes through the center of the primary mirror (point P_1 on Fig. 2). Since the velocity of the mirror surface is perpendicular to its normal at P_1 , the Newtonian and relativistic reflection laws and images of that light ray coincide.

$a_L \setminus a_C$	$\delta a_L \times 10^{-3} \mu\text{as}$			$\delta a_C \times 10^{-3} \mu\text{as}$		
	$-30'$	$0'$	$+30'$	$-30'$	$0'$	$+30'$
$-30'$	0.8239	0.8239	0.8239	0.0003	0.0000	-0.0003
$0'$	0.8236	0.8236	0.8236	0.0000	0.0000	0.0000
$30'$	0.8239	0.8239	0.8239	-0.0003	0.0000	0.0003

Table 1. Angular shifts of the photocenters of aberration patterns due to Special-relativistic effects in the reflection law for the single parabolic mirror rotating at $\Omega = 60''/\text{s}$. The shifts are larger in the along scan a_L direction. The nearly 0 values for δa_C are expected due to the symmetry of the contributions of different light rays in the direction along the angular velocity vector. This symmetry can also be observed aberration patterns of Fig. 3. The effect essentially consists of a constant shift of $\delta a_L \sim 0.0008 \mu\text{as}$ and an utterly small direction-dependent effect $\sim 3 \times 10^{-7} \mu\text{as}$ for both a_L and a_C .

incoming light rays with direction characterized by some given a_L and a_C is generated. These light rays are then traced through the optical system until they intersect the focal plane. The coordinates of the intersection points produce the so-called aberration patterns in the focal plane as it is shown in Fig. 3. The photocenter is defined by averaging the coordinates of the intersection points for each aberration pattern.

It is important to note that the ray tracing discussed in this Section and the next one is performed considering that the photons propagate instantaneously from one surface to the next. This simplification allows us to evaluate the effects of the relativistic reflection law in a clear way

not mixing these effects with the effects of the light propagation time. The finite speed of light propagation also introduces a distortion on the aberration pattern which may be of the same order of magnitude but depends differently on the geometrical and kinematical properties of the optical system. This issue is briefly discussed again in Section 4.3.

The angular shifts obtained for the one-mirror system are shown in Table 1. Since the angle of each light ray with respect to the normal at each point of the surface is no greater than $30'$, the effect of the relativistic reflection law on the aberration pattern is very small. Eq. (67) can be used to estimate the size of the effect. At point P_1 the ve-

locity vector is perpendicular to the normal to the surface. Therefore, at this point for any a_L and a_C the relativistic reflection law coincides with the Newtonian one. A light ray going through that point will intersect the focal plane in the same point in both Newtonian and relativistic cases. The light rays of the same grid not going through P_1 has different images in the Newtonian and relativistic cases. This leads to a shift in position of the photocenters. This shift is however utterly small in the case of the one-mirror system since the individual shifts happen to have an almost null average. The observed weak dependence of the shifts on the focal plane position in Table 1 depends on the shape of the mirror.

4.2. A two-mirror optical system

Real optical systems normally have more than one reflecting surface. Often one has encounters mirrors inclined by about 45° to the optical axis of the primary mirror (i.e., Nasmyth focus, beam combiners, beam splitters, etc.). In this case the relativistic effects on the aberration pattern are much more significant. Here we consider an optical system consisting of one parabolic primary mirror and one flat secondary mirror as depicted on Fig. 4. This flat mirror is inclined an angle θ with respect to the optical axis of the primary mirror. The distance from P_1 to P_2 is $d_{12} = 3$ m, and the distance from P_2 to the center C of the focal plane is $d_f - d_{12} = d_{2f} = 43.67$ m.

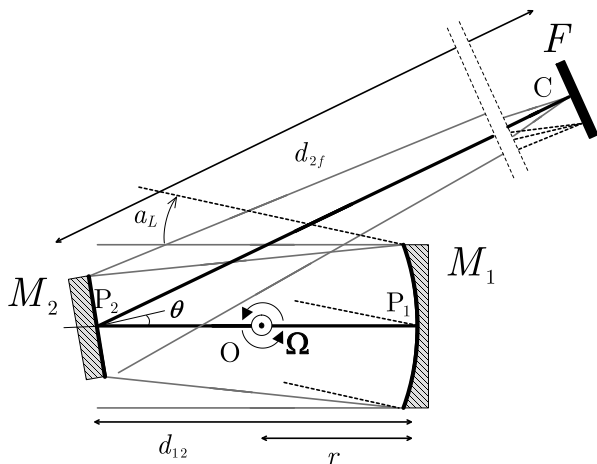


Fig. 4. A flat secondary mirror M_2 has been added to the optical system depicted on Fig. 2. The distance from P_1 to center of the flat mirror P_2 is d_{12} . The focal plane position depends on the angle θ . Now the bold line representing the optical axis goes from P_1 to P_2 and then to the focal plane center C .

We repeat the same ray tracing calculations as in Section 4.1 with this additional flat mirror. We apply three different configurations of the flat mirror using inclination angles $\theta = +45^\circ$, $\theta = 0$, and $\theta = -45^\circ$. Figure 5 shows the aberration patterns obtained with $\theta = 45^\circ$. Clearly,

the relativistic aberration patterns look differently compared to Fig. 3. Numerical values of the shifts δa_L and δa_C are presented in Table 2.

For $\theta = 0$ the obtained shifts are qualitatively very similar to those obtained in the single mirror case. The obtained patterns (not shown here for brevity) show additional but still very small distortions, and the photocenter is barely affected by the presence of this second flat mirror as can be seen from Table 2. Note that the velocity vector is parallel to the surface at the intersection point P_2 of the flat mirror with the *optical axis* like in P_1 (see Fig. 4).

The situation is quite different for $\theta = \pm 45^\circ$. In these cases all the light rays hit the flat surface at an angle of about $\alpha = \pm 45^\circ$ with respect to the normal and the factor $|\sin \alpha|$ appearing in (67) is of the order of $1/\sqrt{2} \approx 0.7$. Each light ray of the grid hits the mirror at slightly different α , but the main relativistic perturbation can be estimated considering the light ray going along the optical axis. Using (67) we obtain

$$\delta_2^O \simeq 2 \frac{\Omega r}{c} \frac{d_{2f}}{d_f} \sin^2 \theta, \quad (79)$$

where d_{2f} is again the distance between P_2 and the focal plane center as it is shown in Fig. 4. One can check that the values of Table 2 for $a_L = a_C = 0$ are recovered from (79) almost exactly. If more flat mirrors are added, the same expression can be generalized as

$$|\delta_i^O| \simeq \left| 2 \frac{v}{c} \frac{d_{if}}{d_f} \sin \alpha_i^O \sin \varphi_i^O \right|, \quad (80)$$

The index i is used to enumerate the surfaces, $i = 1$ corresponding to the primary mirror. In our case $i = 1$ is the parabolic mirror M_1 and $i = 2$ is the flat mirror M_2 . The angle φ_i^O is the angle between the velocity and the surface at the intersection of the mirror M_i with the optical axis, applying the conventions described in Fig. 1. The angle α_i^O is the angle between the optical axis and the normal to the surface at the point of intersection. The quantity d_{if} is the distance from the center of the focal plane C to the point where the optical axis crosses the i -th mirror. As defined above, d_f is the focal distance of the optical system.

The presence of the factor d_{if}/d_f in (79) and (80) can be explained easily. Let us forget about the relativistic reflection law for a moment. Consider that the direction of propagation of a photon p_1 going through the optical axis is slightly perturbed at a distance d_1 from the focal plane. Consider now another photon p_2 that experiences the same perturbation at a closer distance $d_2 < d_1$ from the focal plane. The distances between the photon paths and the optical axis change linearly as the photons propagate toward the focal plane. The rate of this change is the same for both photons. For photon p_2 , which was perturbed closer to the focal plane, the final shift in focal plane coordinates will be smaller than for p_1 by a factor

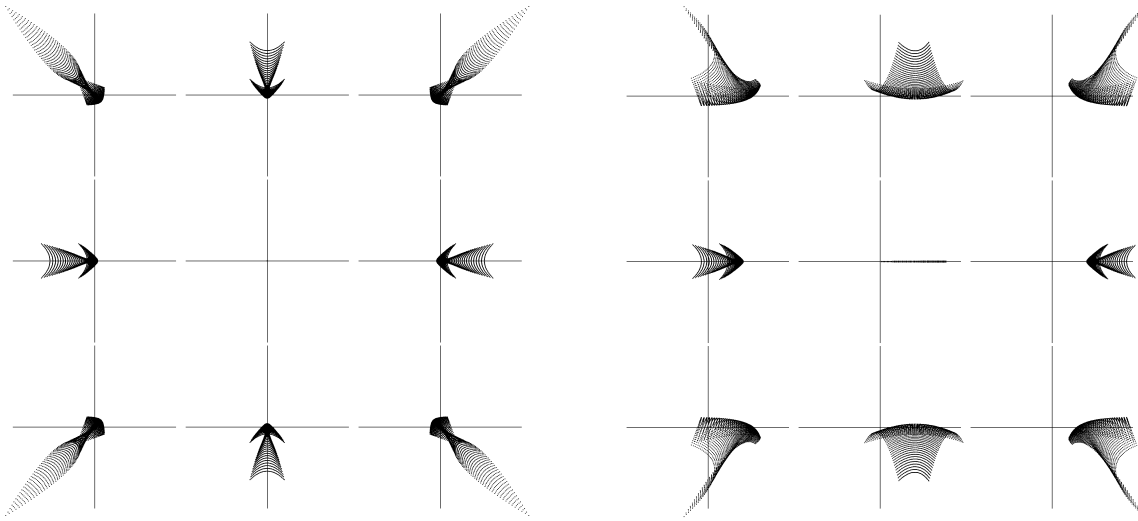


Fig. 5. Aberration patterns obtained for the two-mirror system of Fig. 4 with $\theta = 45^\circ$. The patterns are calculated for the same parameters as for Fig. 2, except for the angular velocity, which now is $\Omega = 500 \text{ s}^{-1}$ (this value is 100 times smaller than the velocity used for Fig. 3). The left panel is again for the aberration patterns for non-rotating instrument ($\Omega = 0$). These patterns are identical to those on the left pane of Fig. 2. From the nine plots of the right pane it can be seen that the patterns are shifted to the right in addition to some distortion of their shapes. This common shift is justified because all the rays, even those going through the optical axis, hit the flat mirror at an angle around 45° and this produces the main relativistic effect common in all of them. Like in the case of the single parabolic mirror, the distortion of the shape of the patterns is due to different velocities of different parts of both mirrors and slightly different incident angles for each mirror. The aberration pattern obtained at $a_L = a_C = 0'$ appears at the central figure of the right pane as thin line around the horizontal axis to the right from the origin. The broadening in the vertical direction a_C clearly seen on Fig. 2 is not seen here since the angular velocity is now 100 times lower.

d_2/d_1 . In the case when $d_1 = d_f$ and $d_2 = d_{if}$ the factor d_{if}/d_f is recovered. In the more general case when the intermediate reflecting surfaces are not flat, Eq. (80) is no longer valid, but gives a reasonable idea of the magnitude of the effect provided that all reflecting surfaces are not too different from a flat mirror.

The cumulative effect of a series of flat mirrors will not be the direct addition of all the δ_i^O since the relativistic perturbation may occur at different planes. An analytic expression in vectorial form can be derived for (80) but the obtained expression is rather complicated and not very useful because it is an approximation valid only for intermediate flat surfaces.

Eq. (80) has been checked also for some other optical systems involving more reflecting surfaces of different shapes, sizes, and velocities. A good agreement with the numbers from numerical ray tracing was obtained in all cases.

4.3. Effects of light propagation delays

As mentioned in Section 4.1, the aberration patterns discussed above were calculated neglecting the finite light propagation time from one optical surface to another. This propagation delays can be indeed totally neglected if the

telescope is not rotating. For a rotating telescope the situation is more complicated and the effect does play a role at least in principle. The effects of the propagation time add additional distortions to the aberration patterns showed above, and blur the effect of the relativistic reflection law. However, since the propagation time effects are not related to relativity, but only with the finiteness of the light velocity, we prefer here to separate them. Since both effects are small, (in the low velocity domain) they can just be added.

The effect of propagation delays can be directly calculated in our software by tracing each individual ray and simultaneously applying the motion of the surfaces. Additionally, each light ray takes different time to cover the distance from the primary mirror to the focal plane, thus obtaining a set of different instants at which the light rays of a given grid hit the focal plane. This means that the light rays producing an aberration pattern hit the primary mirror at different moments of time. Since physical measurement is done at a given moment of time t_{obs} , one must impose that all the light rays producing a pattern hit the focal plane at the same fixed t_{obs} . As a starting point, the different moments of time for each individual light ray are calculated. Then, an iterative process is applied until

$\theta = -45^\circ$ $a_L \setminus a_C$	$\delta a_L \times 10^{-3} \mu\text{as}$			$\delta a_C \times 10^{-3} \mu\text{as}$		
	-30'	0'	+30'	-30'	0'	+30'
-30'	265.6052	265.5951	265.6052	-2.3442	0.0000	2.3442
0'	277.4204	277.4098	277.4204	-2.4271	0.0000	2.4271
30'	289.5789	289.5679	289.5789	-2.5117	0.0000	2.5117

$\theta = 0^\circ$ $a_L \setminus a_C$	$\delta a_L \times 10^{-3} \mu\text{as}$			$\delta a_C \times 10^{-3} \mu\text{as}$		
	-30'	0'	+30'	-30'	0'	+30'
-30'	-0.5567	-0.5567	-0.5568	0.0856	0.0000	-0.0856
0'	-0.6423	-0.6423	-0.6423	0.0000	0.0000	0.0000
30'	-0.5568	-0.5567	-0.5568	-0.0856	0.0000	0.0856

$\theta = +45^\circ$ $a_L \setminus a_C$	$\delta a_L \times 10^{-3} \mu\text{as}$			$\delta a_C \times 10^{-3} \mu\text{as}$		
	-30'	0'	+30'	-30'	0'	+30'
-30'	289.5789	289.5678	289.5789	2.5117	0.0000	-2.5117
0'	277.4204	277.4098	277.4204	2.4271	0.0000	-2.4271
30'	265.6053	265.5951	265.6053	2.3442	0.0000	-2.3442

Table 2. Special-relativistic angular shifts for the optical system described on Fig. 4 rotating at $\Omega = 60''/\text{s}$ and for different inclination angles $\theta = 45^\circ, 0^\circ, -45^\circ$. The behavior of the angular shifts is completely dominated by the effect of the flat mirror when $\theta = \pm 45^\circ$.

all the rays of a pattern collide with the focal plane at this fixed t_{obs} , thus producing the final aberration pattern.

The propagation effects can be also calculated to a good level of approximation using simple geometrical considerations with flat mirrors. There are several effects related to the propagation delays. The first one is just the change of the orientation of the instrument as a whole during the propagation time: an image of a star observed at time t_{obs} is produced by the light rays from the star which hit the primary mirror at time $\sim t_{\text{obs}} - d_f/c$ when the orientation of the latter differed by $\sim \Omega d_f/c$ from the orientation at t_{obs} . The second kind of effects are related to the motion of the focal plane during the propagation delay: during the light propagation the focal plane is moving and the photon hits the focal plane at different position which corresponds to a different position on the sky. The third kind of effects is related to the change of orientations and positions of each intermediate mirror during the propagation from the previous mirror. Although, the effect due to propagation delay can be quite large (e.g. it is about $18 \mu\text{as}$ for the one-mirror system considered in Section 4.1), in many cases the effect only weakly depends on the incident angle. This latter circumstance means that effectively, the propagation delay effects lead only to a constant time shift in the orientation parameters of the satellite derived from astrometric observations: the orientation obtained from observations at t_{obs} is actually the orientation the satellite had some a tiny interval of time earlier. This hardly has consequences on the measurements in any existing or planned astrometric projects.

5. Concluding remarks

We have considered above in detail the main relativistic effect on the imaging by a rotating optical system which is produced by the relativistic change in the reflection law. We have considered two simple optical systems containing one mirror and two mirrors. Although the size of the primary mirror, the focal length and the angular velocity of rotation of both systems were defined to coincide with the corresponding parameters of Gaia, it is not clear how big these effects are for real Gaia optical scheme. We have seen that the effects are utterly small for one-mirror system and that they may amount of $0.3 \mu\text{as}$ for the two-mirror system. For a real Gaia optical scheme the effect may be [much] larger because of the presence of several inclined mirrors. The two examples of a rotating optical system considered above do not allow to predict the relativity-induced photocenter shifts for a real optical system like Gaia. A detailed calculation of the ray tracing shifts can be in principle obtained using the ray tracing software written for this investigation, since all the obtained features (shifts and distortions) are well understood in terms of physical processes. Again the part of the effect which does not depend on the position in the focal plane can be effectively interpreted as a constant change in the orientation of the satellite (as discussed at the end of the previous Section for propagation delay effects). Moreover, if a satellite (like Gaia) has two optically different telescopes, the difference in the main effects for these two telescopes can be interpreted as a change in the angle between the two instruments. It is only the effects depending on the position in the focal plane which really matters for Gaia-like astrometric missions.

In this paper we confined ourselves to ray tracing in the geometric optics limit. A more strict way to analyze the imaging by a rotating optical system is to apply wave optics and calculate corresponding intensity patterns (PSF or similar characteristics). The intensity patterns would then allow to predict the observable shifts of the photocenters more reliably than the aberration patterns used in this paper. Preliminary calculation with a simplified model fosters the hope that at optical wavelengths the differences in the photocenter shifts calculated from the ray tracing and from wave optics are negligible. However, the effects of propagation delays due to the rotation of the telescope may play a role. This may deserve a separate investigation.

References

- Bienaymé, O. & Turon, C. 2002, GAIA: A European Space Project, Vol. textbook (Les Ulis: EDP Sciences)
- Bolotovskii, B. M. & Stolyarov, S. N. 1989a, *Uspekhi Fizicheskikh Nauk*(in russian), 159(1), 155
- Bolotovskii, B. M. & Stolyarov, S. N. 1989b, (in english) *Sov.Phys.Usp.*, 32, 813
- de Boer, K. S., Gilmore, G., E., H., et al. 2000, GAIA: Composition, Formation and Evolution of the Galaxy, Concept and Technology Study Report (ESA-SCI)
- Einstein, A. 1905, *Ann. Physik*, 17, 891
- Gjurchinovski, A. 2004, *Am.J.Phys*, 72, 1316
- Gouda, N., Tsujimoto, T., Kobayashi, Y., et al. 2002, *Ap&SS*, 280, 89
- Hickson, P., Bhatia, R., & Iovino, A. 1995, *A&A*, 303, L37
- Jackson, J. D. 1975, *Classical Electrodynamics* (John Wiley and Sons)
- Klioner, S. A. 2003, *AJ*, 125, 1580
- Klioner, S. A. 2004, *Phys.Rev.D*, 69, 124001
- Lightman, A. P., Press, W. H., Richard, H. P., & Teukolsky, S. A. 1975, *Problem book in Relativity and Gravitation* (Princeton University Press)
- Pauli, W. 1958, *Theory of Relativity* (Pergamon Press)
- Perryman, M. A. C., de Boer, K. S., Gilmore, G., et al. 2001, *A&A*, 369, 339
- Perryman, M. A. C., Lindegren, L., Kovalevsky, J., et al. 1997, *A&A*, 323, L49
- Ragazzoni, R. & Claudi, R. U. 1995, *A&A*, 297, L53
- Shao, M. 1998, in *Proc. SPIE Vol. 3350*, p. 536-540, *Astronomical Interferometry*, Robert D. Reasenberg; Ed., 536-540
- Soffel, M., Klioner, S. A., Petit, G., et al. 2003, *AJ*, 126, 2687